Since January 2020 Elsevier has created a COVID-19 resource centre with free information in English and Mandarin on the novel coronavirus COVID-19. The COVID-19 resource centre is hosted on Elsevier Connect, the company's public news and information website.

CHAPTER

13

DNA markers and nano-biosensing approaches for tuberculosis diagnosis

Amal Rabti, Amal Raouafi and Noureddine Raouafi

Sensors and Biosensors Group, Laboratory of Analytical Chemistry and Electrochemistry (LR99ES15), Department of Chemistry, University of Tunis El Manar, Tunis, Tunisia

List of abbreviations

acpcPNA pyrrolidinyl peptide nucleic acid
AgNPs silver nanoparticles
ALP alkaline phosphatase
AuNPs gold nanoparticles
CFU colony-forming unit
CNTs carbon nanotubes
DPV differential pulse voltammetry
dsDNA double-strand DNA
EC-SERS electrochemical surface-enhanced Raman spectroscopy
E-DNA electrochemical DNA
Exo III Exonuclease III
Fc ferrocenyl groups
FRET fluorescence resonance energy transfer
GF graphene flakes
GOPS 3-glycidoxypropyltrimethoxysilane
HAD helicase-dependent DNA amplification
HPV human papillomavirus
HRP horseradish peroxidase
HRP-Strep streptavidin-horseradish peroxidase conjugate
ITO indium-doped tin oxide
ITS internal transcribed spacer
LAMP loop-mediated isothermal amplification
MBA mercaptobenzoic acid
MBs magnetic beads
MERS-CoV Middle East respiratory syndrome coronavirus
MGIT mycobacteria growth indicator tube
MPs magnetic particles
MSPQC multichannel series piezoelectric quartz crystal
Mtb *Mycobacterium tuberculosis*
MWCNTs multiwalled carbon nanotubes
OMPA oligo-methoxyphenylacetonitrile
PAMAM poly(amidoamine)
PANI polyaniline
PCR polymerase chain reaction
PNA peptide nucleic acid
PPy polypyrrole
QCM quartz crystal microbalance
QDs quantum dots
RCA rolling circle amplification
rGO reduced graphene oxide
rpoB gene responsible for development of resistance to rifampicin
SAM self-assembled monolayers
SPR surface plasmon resonance
SWV square wave voltammetry
TB tuberculosis
tHDA thermophilic helicase-dependent isothermal amplification
TMB 3,3′,5,5′-tetramethylbenzidine

Nanotechnology Based Approaches for Tuberculosis Treatment
http://dx.doi.org/10.1016/B978-0-12-819811-7.00013-8

1 Introduction

Tuberculosis is one of the most serious infectious diseases worldwide with an estimated 10 million new TB cases and a death toll of approximately 1.3 million in 2018 [1]. Despite vaccination and antibiotic treatment available today and that diagnosis and successful treatment of people with TB avert millions of deaths each year, the "end" of TB as an epidemic and a major public health problem remains an aspiration for most countries rather than a reality. Different techniques such as radiometric detection, immunoassays like enzyme-linked immunospot, polymerase chain reaction, TB rapid cultivation detection systems like MB/BacT system, Septi check and BACTEC MGIT system, have been developed in order to reduce the large and persistent gaps in TB detection and treatment [2]. However, these approaches are rather expensive and centralized in large stationary laboratories because they require complex instrumentation with highly qualified technical staff, which make it of paramount importance to construct portable, fast and highly sensitive real-time system for accurate diagnosis and screening of TB infection on time.

As an appealing alternative to conventional techniques, nanotechnology triggered the development of new molecular nanodiagnostic tools with increased sensitivity, specificity, and speed at lower costs. In fact, a variety of nanomaterials-based biosensors have been developed for detection of TB [3,4]. Nano-biosensor is generally defined as a compact analytical device incorporating a biorecognition element with a physicochemical nanometric materials-sized transducer [5]. The biorecognition element, which can be an enzyme, antigen-antibody, nucleic acid, whole cell, etc., is immobilized tightly by different chemical or physical processes onto the transducer that can then measure the arising signals precisely [6].

Here we will provide a closer look into DNA markers used for TB nanodiagnostic and/or *Mycobacterium tuberculosis* (Mtb) detection and characterization. Then, DNA nano-biosensing approaches based on the use of carbonaceous nanomaterials [i.e., graphene and carbon nanotubes (CNTs)] and nanoparticles such as noble metal nanoparticles, metal oxide nanoparticles, magnetic beads (MBs), and quantum dots (QDs) will be described.

2 DNA structure

In order to develop DNA nano-biosensors, the identification and validation of DNA biomarkers for specific sensitive diagnostic of tuberculosis is one of the great challenges to overcome. These biomarkers should be able to identify TB infection in different sample matrixes, such as sputum, plasma, and urine in detectable levels. Moreover, they should be capable to discriminate between infected patients and noninfected subjects [7]. To do so, a single pair of primers can be used as diagnostic markers to detect TB or *Mtb* at a single gene target resolution. Having a very specific target gene does promise high positive predictive values and low false-negative results. However, in terms of analytical sensitivity, a gene with high copy numbers, that is, IS6110 (up to 25 copies in *Mtb* genome), plays an important role in determining the limit of detection of an assay, and thus contributes to higher sensitive diagnostic tests [8]. Chin et al. nicely summarized all the relevant data about DNA targets used for tuberculosis diagnosis in their review [9]. Moreover, they explained the advantages and disadvantages of using each existing marker in Table 13.1. These targets include the rrs (16S rRNA), ITS (16S-23S rRNA), IS6110, groEL2 (hsp65), dnaJ, fbpA (32 kD protein), MPT64 (MPB64), devR, PPE24 (KS4), and lepA genes. Among them, the IS6110 is the most attractive one, as it demonstrates higher sensitivity and specificity due to the multiple copies present in the *Mtb* genome [10].

TABLE 13.1 DNA markers used for TB diagnosis: advantages and disadvantages.

Markers	Advantages	Disadvantages
rrs (16S rRNA)	• Universally used for bacteria identification • Rapid identification of all *Mycobacteria* • Differentiate between *Mycobacterium tuberculosis* complex (MTBC) and tuberculous mycobacteria (NTM) groups • Useful for mutation studies associated with amikacin, kanamycin, and capreomycin resistance	• Insufficient accurate identification of NTM
ITS (16S23S rRNA)	• Identification of the genus *Mycobacterium* • Differentiate between MTBC and NTM • Greater sequence variations than 16S rRNA, which are useful for species differentiation, mainly for NTM	• Unable to differentiate MTBC members
IS6110	• Found exclusively in MTBC in multiple copies • Excellent element for strain genotyping, IS6110-RFLP • High sensitivity and specificity compared to culture and acid-fast bacilli staining in the diagnosis of pulmonary TB	• Low discriminatory power of IS6110-RFLP in isolates with ≤5 IS6110 copies • Unable to differentiate between MTBC members • False positive results with some nonmycobacterium species • False negative results in some MTB strains
groEL2 (hsp65)	• Detected in all mycobacterial strains • hsp65-RFLP can differentiate between MTBC and NTM • Higher accuracy in identification of NTM compared to 16S Rrna	• Lower discriminatory power than dnaJ and fbpA for NTM
dnaJ	• Found in all mycobacteria • Higher discriminatory power than 16S rRNA and hsp65 for NTM	• MTBC members have identical sequence: not suitable for species differentiation
fbpA (32 kDa protein)	• Detected in all mycobacterial strains • Better discriminatory power than hsp65 for NTM	• Identical among MTBC members, not suitable for species differentiation
MPT64 (MPB64)	• Specific for MTBC • Reported useful for TB diagnosis in sputum, ascitic fluid, cerebrospinal fluid, and urine samples • MPB64 PCR is a complement to IS6110 PCR in strains that do not have IS6110	• Might give false positive results in blood samples • False negative results due to mutations in the gene
devR	• Shorter fragments of the gene significantly increased the sensitivity of TB diagnosis	• Lower sensitivity compared to MPB64 and IS6110
PPE24 (KS4)	• High sensitivity and specificity detecting MTBC	• Cross-react with some NTM
lepA	• Useful to identify *Mycobacterium caprae* (specific substitution C690T)	

Reprinted with permission from [9].

3 Carbonaceous nanomaterials-based DNA biosensors

Carbon nanomaterials, such as graphene and CNTs, have been booming for several decades in different fields of applications, especially in analytical and industrial electrochemistry for the investigation of many diseases and their therapy [11,12]. The high surface area of nanoscaled carbonaceous derivatives, their mechanical and electrical properties have made them materials of choice for the manufacture of sensitive, selective and low-cost biosensors for many diseases and especially tuberculosis (Table 13.2).

3.1 Graphene derivatives

Since its discovery in 2004, graphene has been quickly established as a material of choice for many applications in different fields to outshine CNTs, particularly in biosensing applications due to its exceptional mechanical, electronic and optical properties [13]. Chiu et al. developed a novel surface plasmon resonance (SPR) biosensor using graphene nanocomposites-based bioships integrated loop-mediated isothermal amplification for TB biosensing [14]. In fact, SPR relies on the changes of refractive index at the sensor surface in detection applications. The increase in the refractive index is a consequence

TABLE 13.2 Various types of carbon nanomaterials based-DNA biosensors for the detection and identification of tuberculosis.

Signal transduction method	Nanomaterial identity	Samples analyzed	Limit of detection	Linear range	References
Surface plasmon resonance	Graphene	IS6110 of *M. tuberculosis*	Not available	Not available	[14]
	Graphene	IS6110 of *M. tuberculosis*	28 fM	Not available	[15]
Electrochemical response	rGO	DNA from *M. tuberculosis* complex	Not available	Not available	[16]
	rGO	IS6110 of *M. tuberculosis*	50 fM	0.1 pM − 10 nM	[17]
	Graphene	DNA of *M. tuberculosis*	0.015 ng μL^{-1}	0.015–150 ng $/\mu L^{-1}$	[18]
	Graphene	DNA of *M. tuberculosis*	7.853×10^{-7} M	10^{-6} to 10^{-9} M	[19]
	rGO/AuNPs	IS6110 of *M. tuberculosis*	1 fM	$1.0 \times 10^{-15} - 1.0 \times 10^{-9}$ M	[20]
	rGO/AuNPs	DNA of *M. tuberculosis*	0.1 fM	Not available	[21]
	Graphene/Au nanorods	DNA of *M. tuberculosis*	10 fM	10 fM to 0.1 μM	[22]
	GO/CdSQDs	DNA of *M. tuberculosis*	8.948×10^{-13} M	1×10^{-11} to 1×10^{-7} M	[23]
	MWCNTs	rpoB gene of *M. tuberculosis*	0.3 fM	1 fM to 10 pM	[27]
	MWCNTs	rpoB gene of *M. tuberculosis*	Not available	Not available	[30]
	MWCNTs	DNA of *M. tuberculosis*	Not available	Not available	[28]
	CNTs	IS6110 gene of *M. tuberculosis*	0.33 fM	1 fM to 10 nM	[29]
	CNTs/ZrO_2	DNA of *M. tuberculosis*	0.01 nM	1×10^{-2} to 1×10^{-8} mM	[31]
Fluorescence resonance energy transfer	GO	IS6110 of *M. tuberculosis*	Not available	Not available	[24]

of an increase in mass suggesting the occurrence of a binding event. The prepared nanocomposite was constructed of single-layer graphene film deposited onto self-assembled monolayer at a gold electrode. Owing to the strong interactions existing between graphene and DNA, graphene film enabled the detection of Insertion Sequence 6110 (IS611) gene of *Mtb*. The reported results showed high sensitivity and good reliability toward *Mtb* DNA which encouraged the applicability of the SPR-LAMP chip in disease detection.

Recently, graphene was also used by Prabowo et al. for the elaboration of another SPR-based biosensor [15]. A few graphene layers were deposited on top of SPR sensing chip by simple drop casting and used as a platform for DNA probe immobilization. The gold nano urchin tagged-DNA probe was immobilized onto graphene surfaces through π–π stacking interactions. In presence of the target DNA (IS6110), the probe desorbed from the surface to hybridize with its target, which resulted in a variation in the SPR response. The biosensor achieved a detection limit around 28 fM of cssDNA target in salt buffer.

A tremendous body of work has been done to design graphene-based electrochemical biosensor for TB detection. Nguyen et al. described a new approach based on the functionalization of reduced graphene oxide sheets with electroactive copolymer juglone [16]. The hybrid material showed good stability in a biocompatible buffer medium. Moreover, current increase upon hybridization (signal-on) evidenced that short DNA target as well as polymerase chain reaction related to different lineages of *Mtb* strains were successfully detected. The signal-on reached ~40% with 1 nM of short DNA (25 mer) target, while PCR product produced a current change of ~20%.

Polyaniline is another polymer largely used with reduced graphene oxide for biosensing systems. In this context, Chen et al. developed a sandwich-type of *Mtb* DNA biosensor based on the use of polyaniline-reduced graphene oxide, which was decorated with DNA label immobilized onto gold nanoparticles (Fig. 13.1) [17]. The hybridization of the target IS6110 DNA sequence of *Mtb* with its probe leaded to the appearance of a voltammetric signal change resulting from PANI-rGO redox probe. Moreover, the specific IS6110 DNA gene could be detected in the 0.1 pM to 10 nM concentration range, with a detection limit of 50 fM.

As for Mukherjee et al., they have achieved the feat of preparing a 2-dimensional graphene flakes onto indium-doped tin oxide-coated glass plates by electrochemical exfoliation of graphite rods using in situ intercalation of potassium ions [18]. In this approach, the authors modified graphene flakes with a TB DNA probe via amide bond formation between $–CO_2H$ group of GF and $–NH_2$ group of DNA probe. In presence of DNA target, the system responded in the 0.015–150 ng μL^{-1} concentration range with a detection limit of 0.015 ng μL^{-1}.

Furthermore, Mohamad et al. achieved a larger concentration range from 10^{-6} to 10^{-9} M by developing a PANI/Graphene nanofiber platform [19]. The polymerization of aniline monomer and graphene was carried out in the presence of a poly(methyl vinyl ether-alt-maleic acid) solution before the immobilization of a DNA probe related to tuberculosis. Hybridization of the target DNA was monitored by DPV of methylene blue as redox intercalator.

The use of metal nanoparticles, such as gold, with graphene is a very useful way to enhance the biosensing platform metrics. A reduced graphene oxide decorated with AuNPs was exploited by Liu et al. as a sensing platform for the detection of the highly specific tuberculosis biomarker IS6110 in the presence of Au/PANI as a tracer label for signal amplification [20]. The biosensor provided a simple, versatile and powerful tool for reliable diagnosis of *Mtb* over a broad linear range between 10^{-15} and 10^{-9} M.

In the approach developed by Mogha et al., the authors immobilized AuNPs on reduced

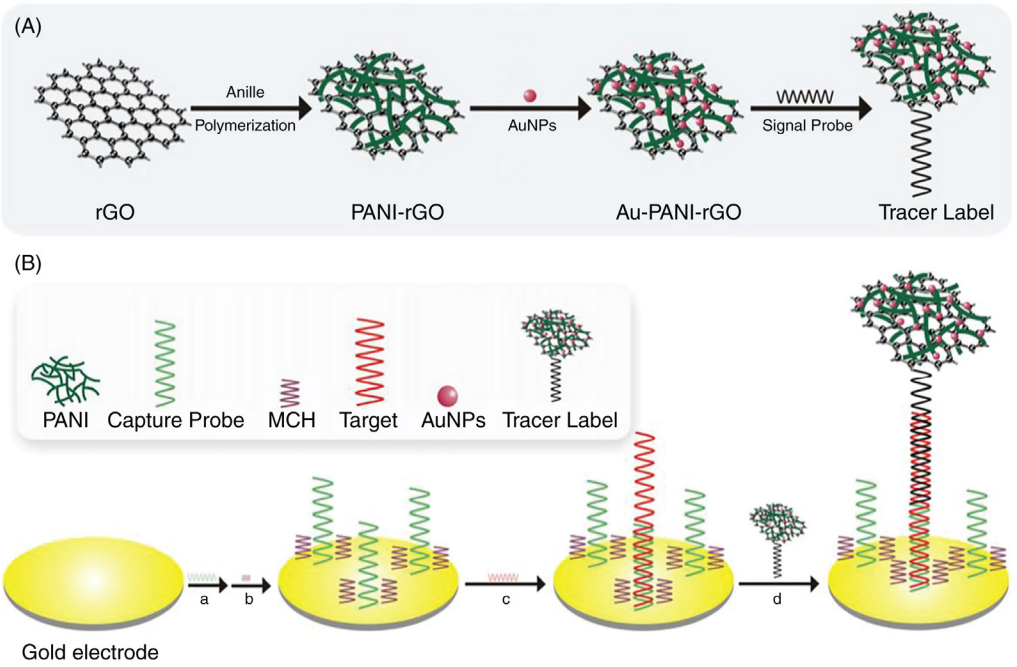

FIGURE 13.1 Schematic representation of the stepwise fabrication process of the electrochemical DNA biosensor. *Reprinted with permission from [17].*

graphene oxide nanoribbons before their functionalization with the DNA probe [21]. Cyclic voltammetry and chronoamperometry were used to quantify the *Mtb* target DNA showing good sensitivity and specificity. Not far from this concept, Perumal et al. prepared another graphene and gold nanocomposite-based biosensor [22]. A 3-D graphene grown by chemical vapor deposition has been modified by gold nanorods obtained from self-assembly of AuNPs on the graphene foam then conjugated to TB DNA probe. The target detection was monitored by electrochemical impedance spectroscopy over a wide detection linear range from 10 fM to 0.1 μM.

Nanocomposite of reduced graphene oxide and CdS QDs were also exploited for the detection of *Mtb*. Zaid et al. introduced CdS QDs to a reduced graphene oxide bearing amine groups before the immobilization of peptide nucleic acid probe [23]. The detection of TB DNA was followed by the DPV signal of methylene blue. The prepared biosensor showed good linearity ranging from 10^{-11} to 10^{-7} M with a detection limit of 8.95×10^{-13} M.

Fluorescence-based biosensors have been attracted great attention from scientific committee these recent years. Usually, when the target concentration is so low, an enzymatic amplification by PCR is essential before or during the analytical process with fluorescence in order to bring the analyte concentration beyond the detection threshold. In this context, Hwang et al. have developed a simple PCR-GO-based system for IS6110 DNA sequence detection [24]. They showed that, in the presence of the target DNA, the results obtained with PCR-GO system using a simple fluorimeter were in agreement with a conventional real-time quantitative PCR results.

3.2 Carbon nanotubes

CNTs were observed for the first time in 1976 by a group of Japanese researchers using a transmission electron microscope [25]. Since their identification in 1991 by Ijima [26], they aroused great interest in several areas thanks to their unique mechanical, thermal, and electronic properties. As an example, they were used by Korri-Youssoufi and collaborators to detect DNA of rpoB gene of *Mtb* [27]. For this purpose, they elaborated a multiwalled carbon nanotubes (MWCNTs) coated with polypyrrole and redox PAMAM dendrimers composite serving as a detection platform (Fig. 13.2). PPy coated MWCNTs acted as transducer and PAMAM dendrimers served to amplify the electrochemical signal. Ferrocenyl groups attached to the surface served as a redox marker. The MWCNTs-PPy-PAMAM-Fc layer was proven as an efficient platform for DNA detection by monitoring the ferrocene redox marker. Cyclic voltammetry and square wave voltammetry demonstrated that the system can detect the target DNA in a large concentration range (1 fM to 100 nM) with low limit of detection. Later on, the same group prepared another MWCNTs-based TB biosensor

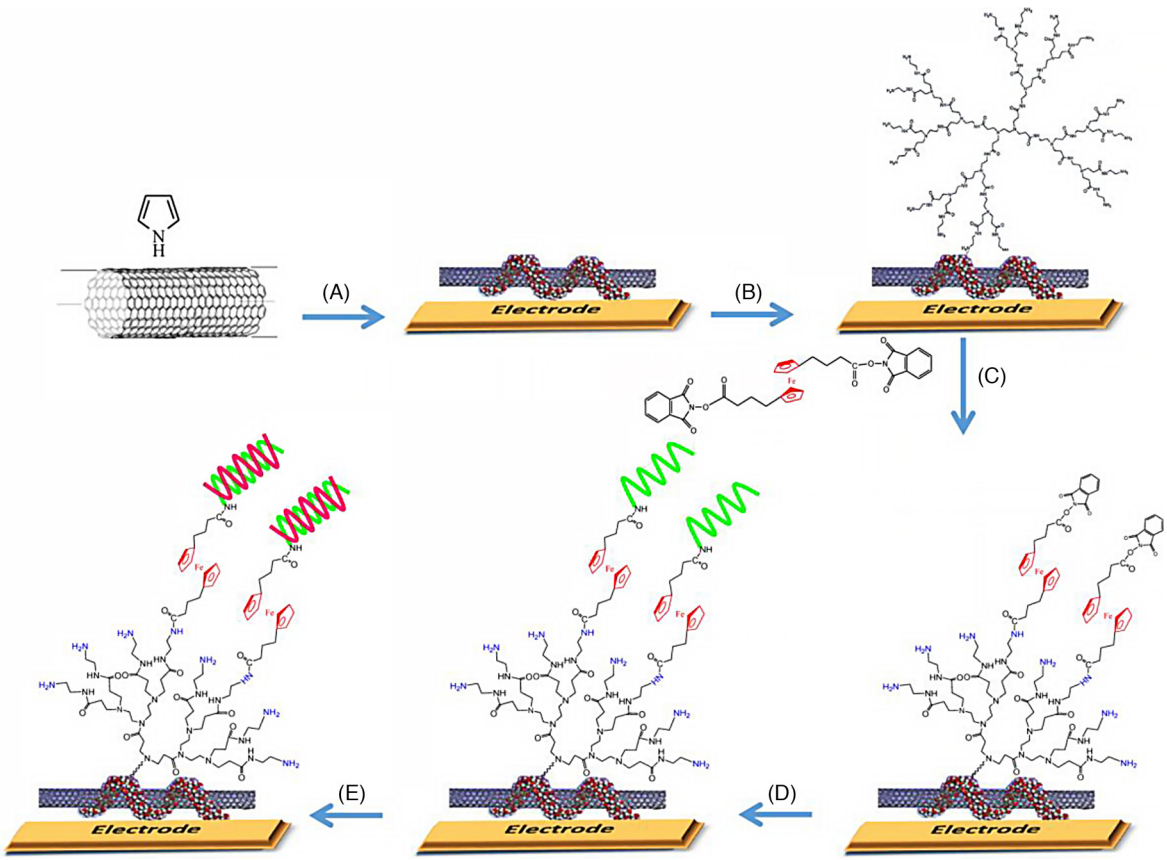

FIGURE 13.2 Schematic illustration of the biosensor elaboration. (A) electropolymerization of pyrrole on MWCNTs, (B) dendrimers attachment through electrochemical oxidation of PAMAM's G4 amines, (C) covalent attachment of ferrocene, (D) covalent attachment of DNA probe, and (E) hybridization with DNA target. *Reprinted with permission from [27].*

using ferrocene modified oligo-methoxy-phenyl-acetonitrile as transducing polymer [28]. This nanocomposite showed high performance of DNA hybridization with a detection limit of 0.08 fM.

The combination of a flower-like CNT with polyaniline was investigated by Chen et al. [29]. In their study, the authors used a rather complicated system with multiple signal amplification strategy in the diagnosis of tuberculosis through DNA detection. The CNTs-PANI nanohybrid was modified with a tracer label to generate the electrochemical signal. The DNA probe hybridization with the target DNA in the presence of an assistant probe yielded a recycling process based on nicking endonuclease-assisted three-way DNA junction process on modified glassy carbon electrode with functionalized fullerene C_{60}. The electrochemical signal had been afforded after hybridization between the cleaved capture probe and the tracer label (Fig. 13.3). The developed biosensor was applicable in a wide linear range (1 fM to 10 nM) with detection limit of 0.33 fM.

Recent advances in electrochemical sensing techniques, combined to microfluidics and nanomaterials, have led to more sophisticated devices. The work of Zribi et al. highlighted the use of microfluidic platform based on MWCNTs modified by ferrocene moieties to detect pathogenic viral Hepatitis C and genomic *Mtb* DNA in clinical isolates [30]. The limit of detection of the reported electrochemical biosensor was enhanced from picomolar in bulk solution to femtomolar in the fluidic device with a wide linear range from 0.1 fM to 1 pM. Moreover, working under high flow, it allowed selective direct detection of rpoB gene of *Mtb* H37Rv from clinical isolate extracted DNA.

Metal oxide nanoparticles were also coupled to CNTs for tuberculosis detection. In fact, Zirconia (ZrO_2) grafted MWCNTs (crystallite size of ZrO_2 ~28nm), obtained via isothermal hydrolysis of zirconium oxychloride in presence

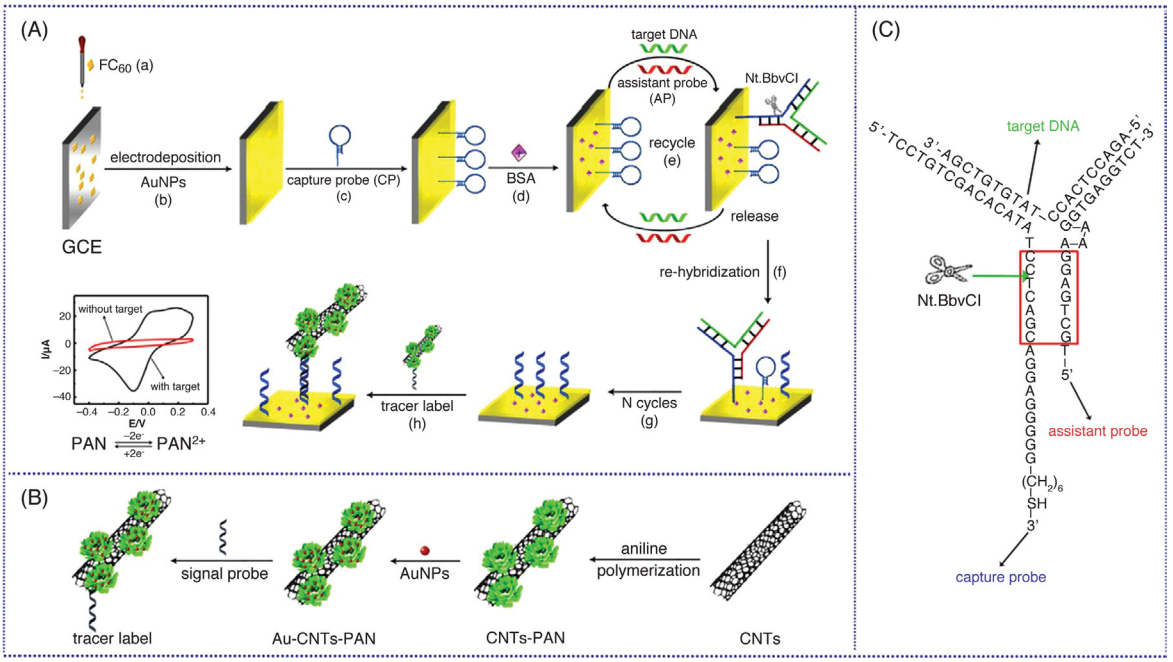

FIGURE 13.3 Schematic representation of the fabrication process of the biosensor. *Reprinted with permission from [29].*

of CNTs, have been electrophoretically deposited onto indium-doped tin oxide-coated glass to develop an impedimetric nucleic acid biosensor for *Mtb* detection [31]. The elaborated nanocomposite applied for IS6110 detection displayed good performances in the concentration range from 10^{-2} to 10^{-8} M with improved detection limit of 0.01 nM.

4 Nanoparticles based-DNA biosensors

Incorporation of nanomaterials and especially nanoparticles with unique properties in biosensing design provided more simple, swift, sensitive and hybrid nano-biosensor platforms with synergetic properties and functions [32]. The intelligent use of such nano-objects led to clearly enhanced performances with increased sensitivities and lowered detection limits of several orders of magnitude, which is due to their high specific surface thus enabling the immobilization of an enhanced amount of bioreceptor units. Moreover, owing to their small size (normally in the range of 1–100 nm), nanoparticles exhibit unique chemical, physical and electronic properties that are different from those of bulk materials, which were used to construct novel and improved biosensing devices. Many types of nanoparticles of different sizes and compositions are now commercially available, which facilitate their application in detection of infectious disease and especially tuberculosis. Table 13.3 summarizes the various types of nanoparticles based-DNA biosensors for the detection and identification of TB.

4.1 Noble metal nanoparticles

Becoming a critical component in the development of nanotechnology-based detection of pathogens, noble metal NPs have attracted considerable attention in molecular diagnostic applications due to their simplicity and versatility [33]. Gold nanoparticles, in particular, have been extensively used due to their easy preparation, inert nature, favorable biocompatibility, high surface area, unique optical properties with their typical bright-red color in colloidal solutions associated with a well-defined SPR band in the visible region of the spectrum, and especially their suitability for binding to biomolecules via thiol-gold association [34].

Colorimetric sensing using gold nanoparticles has been extensively used to detect and characterize pathogens [35] including *Mtb*. These methods rely on the colorimetric changes of the colloidal solution upon aggregation either mediated by a change of the dielectric medium or by recognition of a specific target. The design of these systems is centered in the ability of complementary targets to balance and control inter-particle attraction and repulsion forces, which determine whether AuNPs are stabilized or aggregated and, consequently, the SPR band and color of the solution remains unaltered or changes, respectively. Baptista et al. reported the first application of AuNPs for the molecular diagnostics of *Mtb* by differential stabilization of gold nanoprobes in the presence of different DNA targets [36]. The gold nanoprobes were functionalized with thiol-modified oligonucleotides harboring a sequence derived from the *Mtb* RNA polymerase β-subunit gene sequence suitable for mycobacteria identification. The presence of a complementary target prevented nanoprobe aggregation and the solution remained red, because the nanoprobe solution had a SPR at an absorbance peak of 526 nm, while noncomplementary/mismatched targets or their absence do not prevent gold nanoprobe aggregation at high NaCl concentrations, resulting in a visible change of color from red to blue. The aggregation profile of Au-nanoprobes, and thus identification of specific sequences of *Mtb* complex, namely *Mycobacterium bovis* and *Mtb* in biological samples, was also achieved via the evaluation of the spectra acquired by traditional UV-visible spectrophotometry using a portable and low-cost optoelectronic platform integrating

TABLE 13.3 Various types of nanoparticles based-DNA for the detection and identification of tuberculosis.

Signal transduction method	Nanoparticle identity	Samples analyzed	Detection limit	Linear range	Detection time	References
Colorimetric sensing	AuNPs	DNA of M. tuberculosis	0.75 μg	Not available	2 h	[36]
	AuNPs	DNA from *M. tuberculosis* complex	50 fmol μL^{-1}	50–300 nM	3 h	[37]
	AuNPs	178 bp of IS6110 of *M. tuberculosis*	5 pg	Not available	1 h	[38]
	AuNPs	DNA of *M. tuberculosis*	90 ng	Not available	30 min	[39]
	AuNPs	*M. tuberculosis* complex/rpoB	Not available	Not available	Not available	[40]
	AuNPs	123 bp IS6110 of *M. tuberculosis* dsDNA	1.95×10^{-2} ng mL^{-1}	1.95×10^{-2} to 1.95×10^{1} ng mL^{-1}	60 min	[41]
	AgNPs	DNA of *M. tuberculosis*	1.27 nM	50–2500 nM	Not available	[52]
Surface plasmon resonance	AuNPs	DNA from *M. tuberculosis* complex	10^4 CFU mL^{-1}	10^4 to 10^8 CFU mL^{-1}	40 min	[43]
	AuNPs	rpoB gene of *M. tuberculosis*	Not available	Not available	Not available	[44]
Quartz crystal microbalance	AuNPs	IS6110 of *M. tuberculosis*	5 pg	Not available	Not available	[45]
	AuNPs	16S rDNA fragment from *M. tuberculosis*	20 CFU mL^{-1}	10^2 to 10^8 CFU mL^{-1}	<3 h	[46]
Electrochemical response	AuNPs	105 bp of IS6110 of *M. tuberculosis*	0.01 ng μL^{-1}	Not available	6 h	[47]
	AuNPs	H37rv strain from *M. tuberculosis*	1.25 ng mL^{-1}	1.25–50 ng mL^{-1}	Not available	[48]
	Fe_3O_4	DNA of *M. tuberculosis*	0.1 fM	10.0–200 pg μL^{-1}	Not available	[55]
	Fe_3O_4	DNA of *M. tuberculosis*	6 ng μL^{-1}	5–40 ng μL^{-1}	Not available	[56]
	Fe_3O_4	rpoB gene of *M. tuberculosis*	1 fM	1 fM to 0.1 pM	30 min	[57]
	ZrO_2	DNA of *M. tuberculosis*	0.065 ng μL^{-1}	0.065–640 ng μL^{-1}	60 s	[59]
	ZrO2	DNA of *M. tuberculosis*	0.00078 μM	0.00078–0.05 μM	Not available	[60]
	Magnetic beads	84 bp of IS6110 of *M. tuberculosis*	0.5 aM	0.5–100 aM	<4 h	[61]
	Magnetic beads	ESAT-6 gene of *M. tuberculosis*	1 CFU	Not available	75 min	[62]
	CdSeQDs	DNA of *M. tuberculosis*	8.7×10^{-15} M	1.0×10^{-14} to 1.0×10^{-9} M	50 min	[68]
Electrochemical surface-enhanced Raman spectroscopy	AgNPs	IS6110 of *M. tuberculosis*	280 μg μL^{-1}	Not available	Not available	[51]
Fluorescence resonance energy	CdSeQDs/ magneticbeads	DNA from M. tuberculosis complex	12.5 ng	–	Not available	[65]
	CdTeQDs/AuNPs	ESAT-6 gene of M. tuberculosis	10 fg	Not available	Not available	[66]

a double color tuned light-emitting diode as light source, an amorphous/nanocrystalline silicon photodetector with a flat spectral response in the wavelength range from 520 to 630 nm and integrated electronic for signal acquisition and conditioning constituted by current to voltage converter, a filter and an amplification stage, followed by an analog to digital converter, with appropriate software for full automation to minimize human error [37].

Later, AuNPs modified with thiol oligonucleotide probe, changed color 5 min after hybridization with a loop-mediated isothermal amplified 178 bp sequence of IS6110 DNA of *Mtb* target [38]. Increasing salt concentration of $MgSO_4$ induced the aggregation of the AuNPs probes that was successfully able to detect *Mtb* standard strain till 5 pg of genomic DNA. The same salt-induced aggregation principle was used by Bernacka-Wojcik and co-workers who developed a bio-microfluidic platform for colorimetric *Mtb* DNA analysis based on gold nanoparticles [39]. Their developed platform, consisting in a disposable low cost bio-microfluidic chip with optical fibers and a nondisposable host device integrating light sources, photodetectors, and electronic equipment, required only 3 μL of solution of DNA concentration of 30 ng μL^{-1} (90ng), which allowed 20-fold reduction of the needed volume compared to the bulk version of this biosensor and 10-fold reduction when compared with the microplate reader reference method.

Following a noncrosslinking colorimetric methodology, Veigas et al. demonstrated that a single gold-nanoprobe was capable to detect both members of the *Mtb* complex and *Plasmodium* sp., the etiologic agents of tuberculosis and malaria, relying on the differential aggregation profile of Au-nanoprobes following an increase of the ionic strength of the medium (e.g., salt addition, $MgCl_2$) [40]. The developed gold-nanoprobe allowed detection of either target in individual samples or in samples containing both DNA species with the same efficacy. Moreover, a colorimetric sensing strategy employing gold nanoparticles and a paper-based analytical platform was developed by utilizing the SPR effect to monitor changes in the color of a gold nanoparticle colloid before and after hybridization of single-stranded DNA probe molecules with targeted double-stranded tuberculosis DNA [41]. The hybridization event changed the surface charge density of the nanoparticles, causing them to aggregate to various degrees, which modified the color of the solution in a manner that can be readily measured to determine the concentration of the target DNA. The adapted method, consisting on a label-free oligonucleotide and unmodified gold nanoparticle solution-based technique, was extended to a paper-based system that can be measured using a smart phone to obtain rapid parallel colorimetric results with low reagent consumption and without the need for sophisticated analytical equipment. Multiple tests were performed simultaneously with a 60 min turnaround time with a detection limit of 1.95×10^{-2} ng mL^{-1}.

AuNPs are known to induce a considerable shift in the angle of plasmon resonance which makes them suitable nanomaterial for the investigation of SPR-based biosensors. These biosensors are surface-sensitive analytical tools based on the ability to detect changes in the refractive index that are caused by the interaction between an analyte and a biological recognizer immobilized on the biosensor surface [42]. Xiang et al. developed SPR DNA biosensing arrays to rapidly and accurately detect *Mtb* complex and *Mycobacterium avium* complex in parallel, through the integration of liquid RCA reaction (Fig. 13.4) [43]. A sequence in 16S-23S rRNA gene internal transcribed spacer was targeted by the designed species-specific padlock probe. Hybridization analysis of ITS gene allowed the real-time monitoring of target-primed RCA in liquid-phase with AuNPs-embedded SPR sensing method. Taking advantage of the specificity of padlock probes, the simplicity of

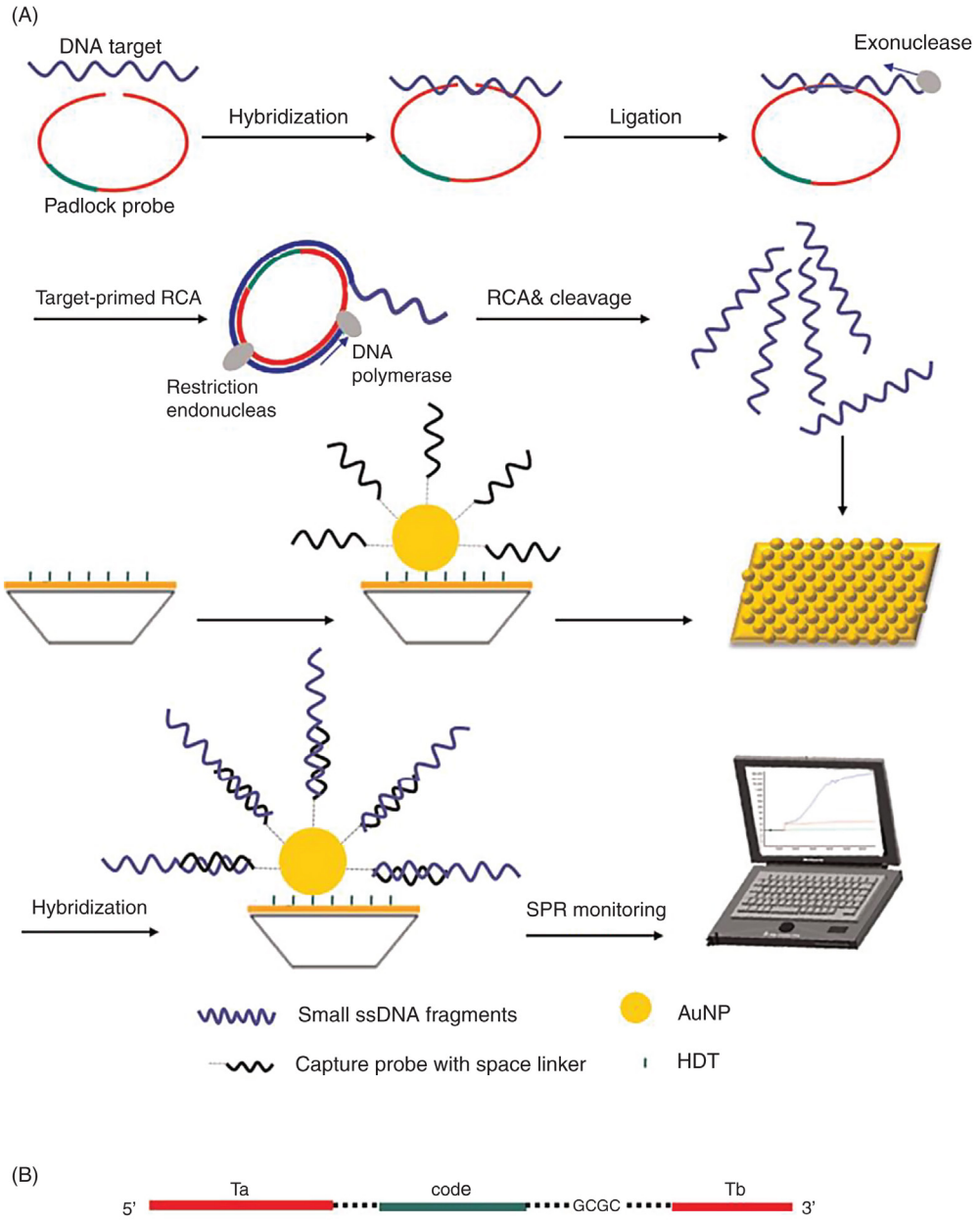

FIGURE 13.4 (A) The principle of the target-primed RCA-cleavage reaction-based AuNP-embedded SPR assay. (B) The mode of the padlock probe. Ta and Tb are asymmetric target complementary regions in the PLP. Each PLP contains a unique code sequence for multiplex hybridization. The *dotted line* represents the bases in the linker sequence. *Reprinted with permission from [43].*

target-primed RCA, the combination of RCA and digestion reaction, and the enhanced sensitivity of AuNPs-embedded SPR sensor, provided improved detection limit with high fidelity. In another research, gold nanoparticles modified by thiolated DNA were used for selective amplification up to ~1200 times of SPR biosensor signal for recognition of rpoB gene of *Mtb* [44]. The light extinction was fixed at 520 nm, considered as a measure of a quantity of the nonaggregated gold nanoparticles, to investigate the influence of the ionic strength on the aggregation stability of unmodified and oligonucleotides-modified AuNPs.

Combined with quartz crystal microbalance biosensor, gold nanoparticle amplification appeared to be a suitable and convenient tool for *Mtb* diagnosis [45]. In fact, hybridization of IS6110 amplified DNA target sequence, modified at 3′ end with AuNPs as mass enhancement, to the probe oligonucleotide immobilized onto gold electrode of the quartz crystal were studied through the changes in QCM frequency, which indicated that the developed biosensor could detect serial dilution of *Mtb* DNA limited to 5 pg of genomic DNA. Recently, Zhang et al. reported the use of a 16S rDNA multichannel series piezoelectric quartz crystal sensor based on Exonuclease III-aided target recycling for rapid detection of *Mtb* H37Ra strain (Fig. 13.5) [46]. The specific 16S rDNA fragment of *Mtb* was used as biomarker while DNA capture probes complementary to the biomarker were designed and modified on the surface of AuNPs. The Exo III which could recognize hybrid duplexes and selectively digest DNA capture probe was used to assist digestion cycle by digesting DNA capture probe and releasing the intact target fragment. After all DNA probes loading on the surface of AuNPs were removed, the surface of AuNPs was exposed and conductive connection was formed between the nanogap network electrode by self-catalytic growth of exposed AuNPs in the glucose and $HAuCl_4$ solution, which resulted in sensitive response of *Mtb* sensor. The limit of detection of the method was 20 CFU mL^{-1} and the detection time was less than 3 h. Moreover, the proposed method was applied to detect *Mtb* in simulated sputum samples with satisfactory results.

Electrochemical AuNPs-based biosensors emerged as an important analytical tool for diagnosis of tuberculosis to converge the demands of high sensitivity and early detection in less time due to the unique tunable physicochemical properties of AuNPs plus their conducting capability and high surface-to-volume ratio. Their mechanism of detection relies on specific changes in electrical signals such as conductance, impedance, potential, and capacitance at a surface-functionalized electrode by either chemical reactions or physical interactions. For example, Torres-Chavolla and Alocilja described the use of thermophilic helicase-dependent isothermal amplification and dextrin coated gold nanoparticles as electrochemical reporter for detection of a fragment within the IS6110 gene (105 bp), which is specific to *Mtb* complex [47]. The biosensor was composed of AuNPs and amine-terminated magnetic particles each functionalized with a different DNA probe that specifically hybridize with opposite ends of the target DNA. After hybridization, the formed complex (MP-target-AuNPs) was magnetically separated from the solution and the AuNPs were electrochemically detected on a screen-printed carbon electrode. The obtained detection limit was 0.01 ng μL^{-1} of isothermally amplified target.

In Thiruppathiraja et al. research, dual-labeled AuNPs was used as a signal amplifier to build an electrochemical biosensor for Mycobacterium sp. genomic DNA detection in a clinical specimen [48]. The electrochemical genosensor was fabricated using a sandwich detection strategy involving hybridization of target DNA to alkaline phosphatase and detector DNA probes dual-labled AuNPs. The electrochemical signal was generated through electroactive para-nitrophenol molecules produced by enzyme catalytic hydrolysis of para-nitrophenol phosphate.

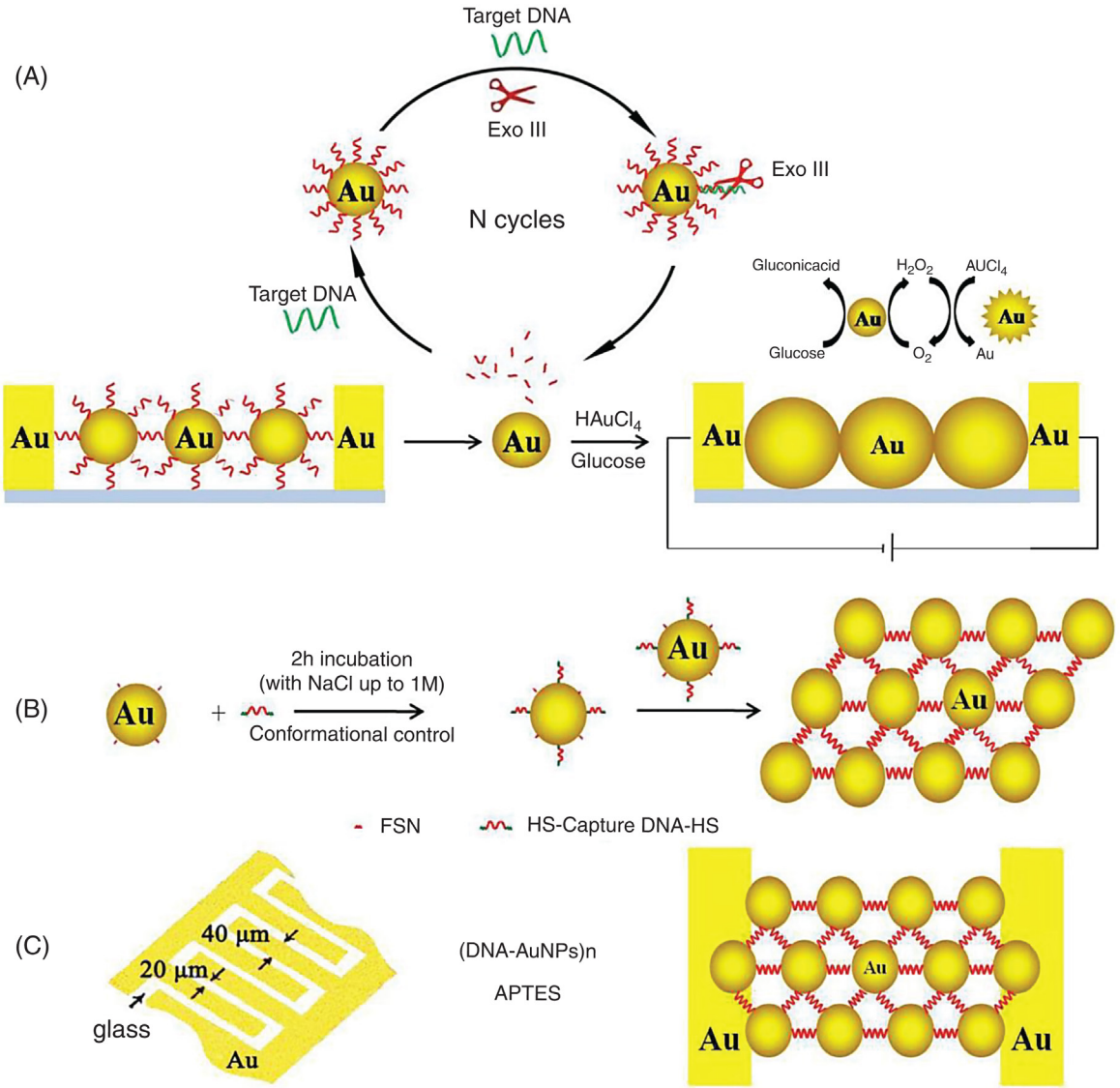

FIGURE 13.5 **The constructed strategy of 16S rDNA MSPQC sensor.** (A) Sensing scheme of the sensor. (B) Preparation method of AuNPs-DNA conjugates. (C) The preparation of AuNPs-DNA network electrode. *Reprinted with permission from [46].*

A detection limit of 1.25 ng mL^{-1} genomic DNA was achieved under optimized conditions. Moreover, the outcome of the developed biosensor in clinical sputum samples was in agreement with the PCR analysis.

Silver nanoparticles (AgNPs) have attracted increasing attention due to their quantum characteristics including large specific surface area, easy preparation and small granule diameter [49]. Additionally, they are also known to have

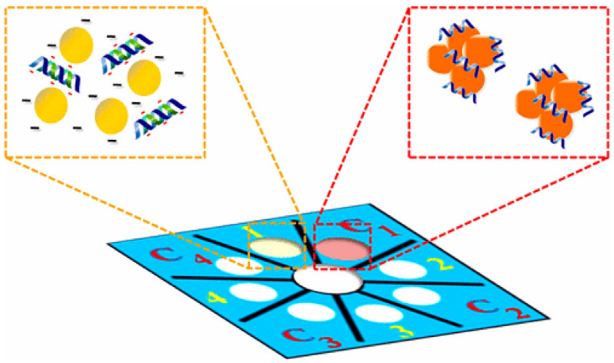

FIGURE 13.6 The process of acpcPNA-induced AgNP aggregation in the presence of complementary DNA and non-complementary DNA multiplex paper-based colorimetric device. *Reprinted with permission from [52].*

a higher extinction coefficient compared to AuNPs [50], which leads to better optical sensitivity. Thus, AgNPs were also employed to construct tuberculosis DNA-based biosensors.

Electrochemical surface-enhanced Raman spectroscopy shows excellent promise for the detection of biological analytes such as DNA bases, nucleotides, and DNA aptamers in aqueous media. Karaballi et al. described the preparation of an EC-SERS DNA aptasensor capable of direct detection of tuberculosis DNA, without the need for costly labels or Raman reporter molecules [51]. Cost-effective screen-printed electrodes modified with silver nanoparticles were used as the aptasensor platform, onto which the aptamer specific for the target DNA was immobilized. In fact, a 5'thiolated probe-target DNA pair chosen such that the target strand, a sequence contained within the IS6110 fragment, contained adenine, while the probe strand did not, was immobilized onto AgNPs surfaces and a complete self-assembled monolayer was prepared by thiol back-filling in order to reduce nonspecific macromolecular adsorption onto the SERS substrate. Incubation with the target strand allowed for direct monitoring of DNA hybridization in synthetic urine via the appearance of the adenine marker bands. Modulation of the applied potential allowed for a sizeable increase in the observed SERS response, likely due to the potential-induced desorption of adsorbed citrate molecules. These experiments were also conducted in synthetic urine, a more realistic electrolyte for detecting urine DNA biomarkers; however, the signal was weaker, most likely due to the presence of chloride.

Recently, Tee-ngam et al. reported the development of a paper-based colorimetric assay for Middle East respiratory syndrome coronavirus, *Mtb* and human papillomavirus DNA detection based on pyrrolidinyl peptide nucleic acid-induced AgNPs nanoparticles aggregation (Fig. 13.6) [52]. In fact, PNA probes are an attractive alternative to DNA and RNA probes because they are chemically and biologically stable, easily synthesized, and hybridize efficiently with the complementary DNA strands. The acpcPNA probe contains a single positive charge from the lysine at C-terminus and causes aggregation of citrate anion-stabilized AgNPs in the absence of complementary DNA. In the presence of target DNA, formation of the anionic DNA-acpcPNA duplex caused the dispersion of the AgNPs as a result of electrostatic repulsion, giving rise to a detectable color change. The oligonucleotide targets were detected by measuring the color change of AgNPs, giving detection limits of 1.53 nM (MERS-CoV), 1.27 nM (*Mtb*) and 1.03 nM (HPV). Moreover, the acpcPNA probe exhibited high selectivity for the complementary

oligonucleotides over single-base-mismatch, two-base-mismatch and noncomplementary DNA targets.

4.2 Metal oxide nanoparticles

Metal oxide nanoparticles have many advantageous properties that make them useful in the transducer component of biosensors. Increased investigations have been carried out with several types of iron oxides nanoparticles. Among them, magnetite Fe_3O_4, ferromagnetic and superparamagnetic when the size is less than 15 nm, is very promising and popular candidate since its biocompatibility have already been proven [53]. Due to their small size, large surface-to-volume ratio, high chemical activity and biological compatibility, Fe_3O_4 nanoparticles have attracted more attention for biomedical applications in the field of biosensors [54].

Combined to 3-glycidoxypropyltrimethoxysilane, Fe_3O_4 nanoparticles were used to form a biocompatible matrix onto hydrolyzed indium-doped tin oxide glass plate for immobilization of *Mtb* specific 21-mer peptide nucleic acid probe for hybridization detection [55]. SWV was applied to study the electrochemical response of the prepared electrode with and without Fe_3O_4 in the presence of complementary, noncomplementary and one-base mismatch DNA using methylene blue as an electrochemical indicator. The PNA/Fe_3O_4-GOPS/ITO electrode was used to detect the hybridization with the complementary sequence in sonicated *Mtb* genomic DNA within 90 s of hybridization time. Moreover, it showed improved specificity and detection limit (0.1 fM) as compared to that of the PNA-GOPS/ITO bioelectrode (0.1 pM), which was due to the presence of magnetic nanoparticles as they promote faster mobility to electrons generated during response measurements.

Costa and co-workers reported the fabrication of a genomic DNA from *Mtb* genosensor based on the use of bare Au electrode modified with self-assembled monolayers of mercaptobenzoic acid and magnetite nanoparticles [56]. The cysteine-coated magnetic Fe_3O_4 nanoparticles were linked via the carboxylate group from MBA to the work electrode surface and subsequently to the DNA probe. The probe-target interaction was investigated using $Fe(CN)_6^{3-}/Fe(CN)_6^{2-}$ as a redox pair probe. Changes in the charge transfer resistance were registered after interaction of the sensor with different concentrations of genome DNA. The impedimetric response increased with increasing target DNA concentrations. Moreover, a detection limit of 6 ng μL^{-1} was achieved.

Combining the catalytic properties of iron oxide nanoparticles with conducting properties of polypyrrole platform, the selective detection of wild and mutated rpoB gene in *Mtb* was achieved using an electrochemical DNA sensor based on polypyrrole/Fe_3O_4 nanocomposite bearing redox naphthoquinone tag on PAMAM dendrimers (Fig. 13.7) [57]. The decrease of the electrochemical signal response of the attached naphtoquinone was used to follow the hybridization. The fabricated biosensor was able to detect up to 1 fM of DNA target in a 50 µL drop corresponding to 3×10^4 copies of DNA. Moreover, it was applied to selectively detect and discriminate wild type DNA from mutated DNA strands of *Mtb* in both PCR amplified samples and samples without PCR amplification. Therefore, the amplification procedure could be avoided with this biosensor which also offered the possibility of measurements using drop size samples opening the possibility to their use as point-of-care system for *Mtb* detection and drug resistance discrimination.

Among the large number of nanostructured metal oxides that have been explored for application in electrochemical biosensors, Zirconia has attracted much attention because of its thermal stability, chemical inertness, biocompatibility, and affinity for the groups containing oxygen [58]. Das et al. have reported the use of these nanoparticles for the construction of *Mtb* electrochemical DNA based-sensors [59,60]. After being electrochemically deposited onto gold surface, nanostructured ZrO_2 film (particle size

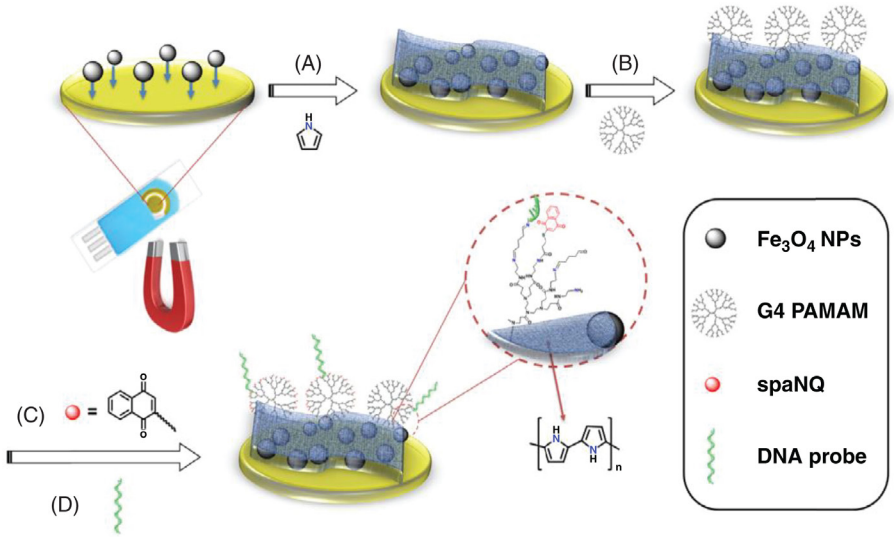

FIGURE 13.7 Design method of electrochemical DNA (E-DNA) sensor based on polypyrrole/Fe_3O_4 nanocomposite bearing redox naphthoquinone tag on PAMAM dendrimers for ropB gene DNA sensing: (A) electrochemical magneto-polymerization of F_33O_4 NPs/pyrrole, (B) electrochemical grafting of PAMAM, (C) naphtoquinone (spaNQ) coupling, and (D) functionalization by the DNA probe. *Reprinted with permission from [57].*

~35 nm) were used to immobilize a 21-mer oligonucleotide probe ssDNA specific to the bacteria through the affinity between oxygen atom of phosphoric group and zirconium (Fig. 13.8) [59]. The resulted electrode was able to detect the target DNA within 60 s in the range from 640 to 0.065 ng μL^{-1} with detection limit of 0.065 ng μL^{-1} for target DNA concentration and of genomic DNA as low as 1 ng μL^{-1}. Electrophoretically fabricated nanostructured chitosan-zirconium-oxide composite film (180 nm) onto ITO-coated glass plate was applied as an adhesion layer for the investigation of DNA hybridization [60]. The morphological studies clearly revealed uniform inter-linking and dispersion of hexagonal nanograins of ZrO_2 (30–50 nm) into the chitosan matrix, resulting in homogeneous nanobiocomposite formation. After covalent immobilization of biotinylated probe DNA specific to *Mtb*, electrochemical response measurements of the prepared bioelectrode showed that it was selective and can detect complementary target up to 0.78 nM with sensitivity of 6.38×10^{-9} A nM^{-1}.

4.3 Magnetic beads

MBs were used to quantify an 84-bases long sequence specific of *Mtb* based on coupling asymmetric helicase-dependent DNA amplification, post-amplification hybridization and electrochemical enzyme-mediated detection (Fig. 13.9) [61]. To overcome the unspecific amplification problems associated to most isothermal nucleic acid quantification strategies, selecting an asymmetric format for HDA was applied and an amplification factor of $>10^6$ folds was achieved. Then, the relatively short single-stranded amplicons (80–120 bp) obtained in HDA were trapped onto MBs and detected by hybridization to a fluorescein-tagged probe, which improved the assay selectivity. Under isothermal conditions, *Mtb* gene was quantified in less than 4 h down to 0.5 aM, corresponding to 15 copies of the target gene in 50 µL of sample, three orders of magnitude below the limit of detection of a real-time fluorescence HDA system. Moreover, *Mtb* was successfully detected in sputum, pleural fluid and urine samples.

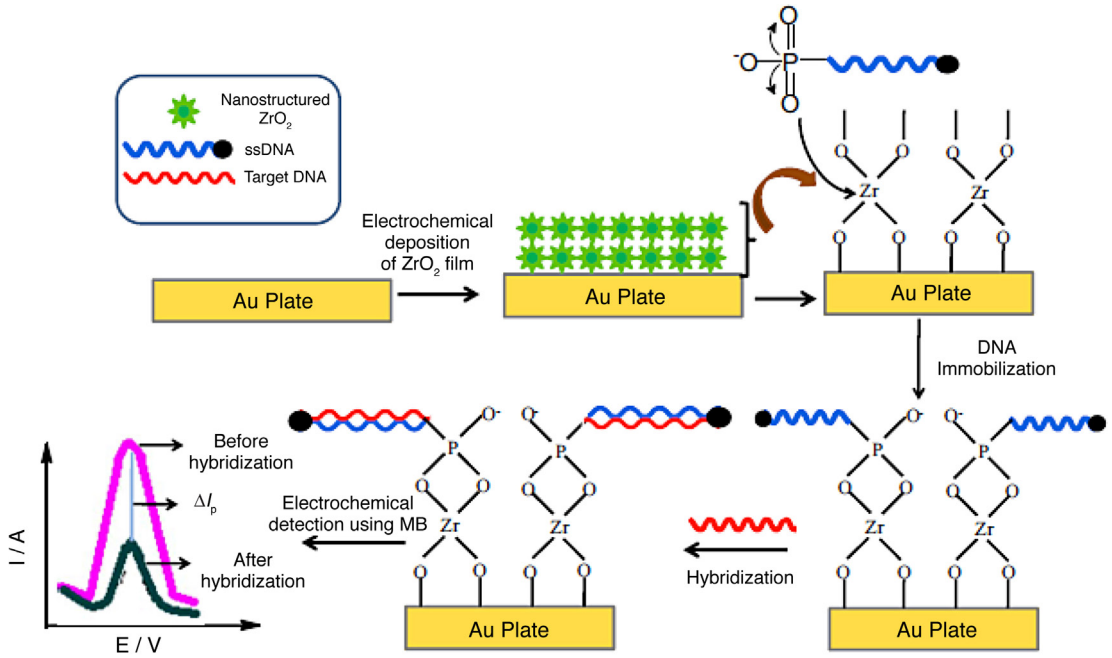

FIGURE 13.8 **Proposed schematic for the fabrication of nanoZrO_2/Au based DNA biosensor.** *Reprinted with permission from [59].*

Ng et al. developed a highly specific colorimetric biosensor to detect isothermally amplified *Mtb* DNA by the catalytic oxidation of 3,3′,5,5′-tetramethylbenzidine with horseradish peroxidase at a sensitivity approaching the genomic equivalent of a single *Mtb* colony forming unit [62]. Moreover, as TMB is an electroactive material [63], the developed biosensor was also adapted onto commercially available disposable screen-printed carbon electrodes, to demonstrate an alternative electrochemical quantification method for *Mtb* detection. To this end, amplified DNA samples were simultaneously incubated with streptavidin and streptavidin-HRP-coated MBs, which would competitively bind with available biotin handles within the DNA amplicons. After being separated using a magnetic plate and all unbound HRP-Strep were removed through washing, TMB substrate was added to react with any captured HRP. The intensity of the colored TMB substrate was likely proportional to the amount of amplified biotinylated DNA, which is in turn proportional to the amount of *Mtb* DNA originally present. Positive assay results were then visualized with the naked eye, quantified with spectrometry or electrochemically using SPCEs and a portable potentiostat. The assays were inexpensive (US$3), rapid (75 min), and sensitive (approaching single cell). Moreover, they were also highly specific to *Mtb* due to the use of the ESAT-6 gene as a *Mtb*-specific molecular target. The simplicity of naked eye interpretation, eliminating the need for sophisticated equipment not always available, was an added advantage for point-of-care analysis.

4.4 Quantum dots

QDs have been widely utilized because of their characteristics of signal enhancement, inherent miniaturization, low detection limits,

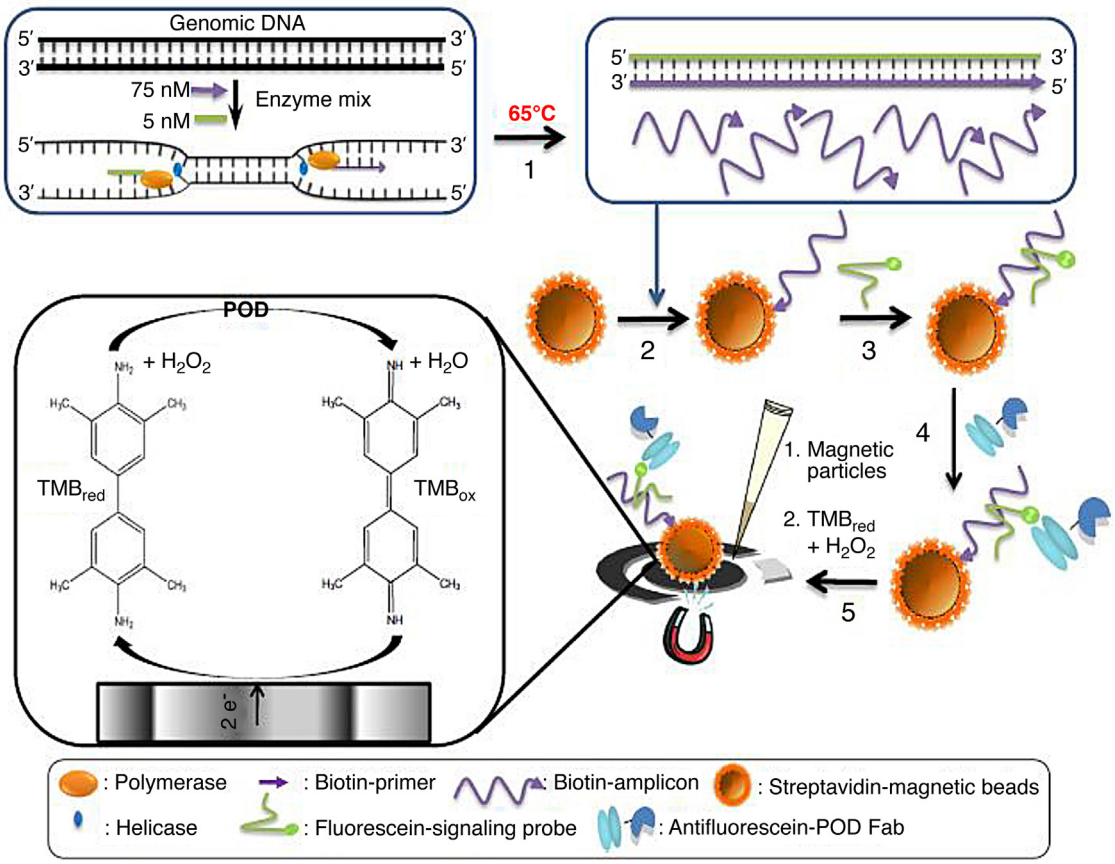

FIGURE 13.9 Overview of the different steps of the asymmetric HDA-electrochemical-genomagnetic assay. *Reprinted with permission from [61].*

low-cost, low power requirements, and especially because they have excellent stability against environment and chemicals. They are considered as one of the most attractive fluorescent semiconductor nanocrystals that can be used as alternative fluorescent probes for their unique optical properties such as high fluorescence yields, high photo-stability and narrow symmetric emission spectrum [64]. Cases in point, the QDs were used as biosensors for *Mtb* DNA detection.

Gazouli and co-workers developed and evaluated a specific DNA detection method using fluorescent semiconductor QDs and MBs for fast detection of two members of the *Mycobacterium* genus (*M. tuberculosis* and *M. avium* subsp. paratuberculosis), dispensing with the need for DNA amplification [65]. To do so, two biotinylated oligonucleotide probes, designed based on IS6110 and IS900, were used to recognize and detect specific complementary mycobacterial target DNA through a sandwich hybridization reaction. CdSe QDs conjugated with streptavidin and species-specific probes were used to produce a fluorescent signal, while the MBs conjugated with streptavidin and a genus-specific probe were used to isolate and concentrate the DNA targets. The minimum detection limit of the

assay was defined as 12.5 ng of DNA diluted in a sample volume of 20 μL. The optimized assay was applied to the detection of *Mtb* in DNA isolated from bronchoalveolar lavage specimens from patients with tuberculosis and *M. avium* subsp. paratuberculosis in DNA isolated from feces and paraffin-embedded tissues. Moreover, the system was compared with conventional diagnosis methodologies, namely Ziehl-Neelsen staining and real-time PCR. The concordance of these methods compared to the proposed method with regard to positive and negative samples varied between 53.84% and 87.23% and between 84.61% and 100%, respectively. The overall accuracy of the QDs assay compared to real-time PCR was 70%–90% depending on the type of clinical material. Additionally, the method avoided the drawback of PCR-based diagnostic assays that are prone to false-negative results generated by inhibitors commonly found in clinical samples such as feces. Given that the capture and detection probes of the QDs assay are complementary to different genes of the mycobacterial genome, which give rise to false-negative results due to the increase of the DNA fragmentation, the use of a different set of DNA probes that anneal closer to each other, allowed an assessment that minimizes false-positive results associated with low specificity.

A sandwich-form fluorescence resonance energy transfer-based biosensor was developed to detect Mtb complex and differentiate *Mtb* and *M. bovis* Bacille Calmette-Guerin simultaneously, based on the use of a surface-modified cadmium-telluride QDs and gold nanoparticles conjunct with two specific oligonucleotides against early secretory antigenic target 6 (Fig. 13.10) [66]. The sensitivity and specificity of the prepared biosensor were 94.2% and 86.6%, respectively, while the sensitivity and specificity of polymerase chain reaction and nested polymerase chain reaction were considerably lower, 74.2%, 73.3% and 82.8%, 80%, respectively. The detection limits were far lower (10 fg) than those of the PCR and nested PCR (100 fg). Despite that the cost of the developed nanobiosensor was slightly higher than those of the PCR-based techniques, the speed, the higher sensitivity and specificity, as well as a 10-fold lower detection limit, the large-scale application of FRET-based biosensor would be more cost-effective.

QDs have received more attention because the signal response could be generated from QDs themselves [67]. In fact, CdSe QDs were applied as signal markers to detect *Mtb* DNA [68]. The developed electrochemical biosensor was designed using CdSe QDs as a label combined with MspI endonuclease and AuNPs to improve the selectivity and amplify the signal. A molecule of MspI endonuclease has a molecular mass of 29 kDa [69]. It recognizes the duplex symmetrical sequence 5′-CCGG-3′ and catalyzes the double-strand DNA cleavage between the two cytosines but does not act on single-strand DNA. It easily cleaved the dsDNA fragments linked with CdSe QDs from the electrode, resulting in a decrease in the electrochemical signal. The remaining attached CdSe QDs were read out by SWV using an electrodeposited environmentally friendly bismuth film-modified glass carbon electrode. The higher the concentration of target *Mtb* DNA, the lower the electrochemical signal. Based on the variation of current before and after digesting the DNA hybrid, a novel signal-off electrochemical DNA biosensor was developed. Under the optimal conditions, the proposed biosensor detected *Mtb* DNA down to 8.7×10^{-15} M with a linear range of five orders of magnitude (from 1.0×10^{-14} to 1.0×10^{-9} M) and discriminated mismatched DNA with high selectivity.

5 Conclusion

Access to cheaper and reliable TB diagnosis is one of the ultimate goals to be accomplished by scientists and urgently needed for TB fight worldwide. Given that conventional diagnostic techniques for this disease like culture and

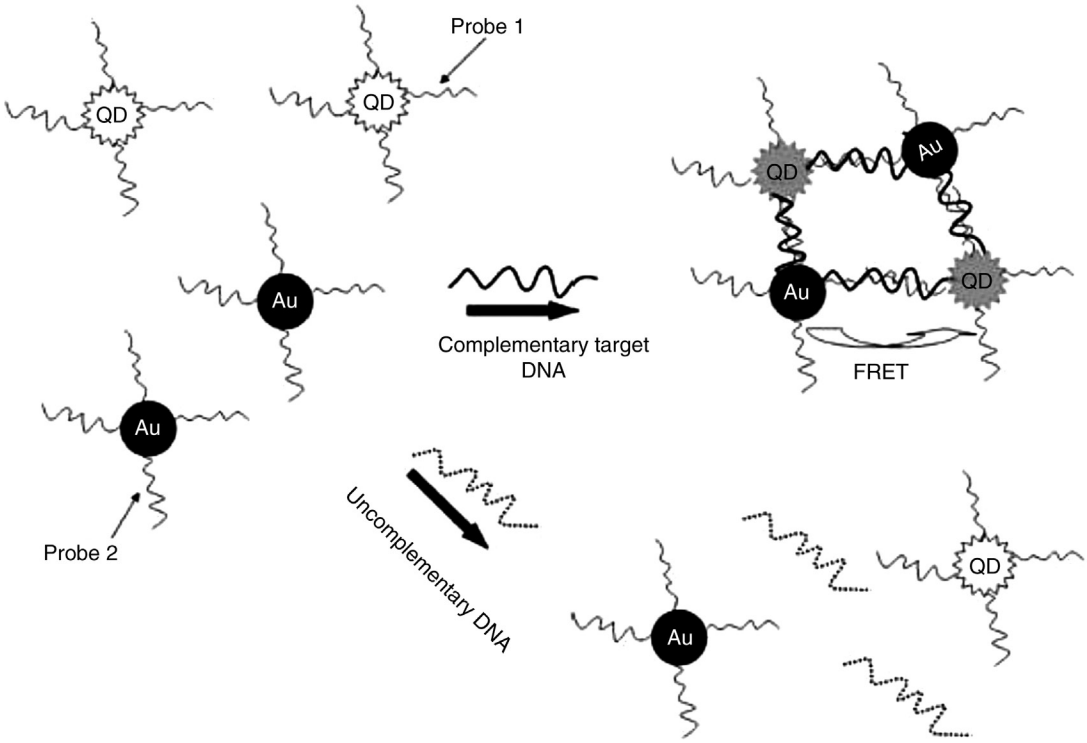

FIGURE 13.10 Sandwich-form FRET-based biosensor schematic. In the presence of the target the AuNPs/P2 moiety optically quenched the QDs/P1 moiety. Presence of the target molecules turned the AuNPs/P2 into a fluorescence acceptor close enough to the QDs/P1 resulting in a FRET signal. *Reprinted with permission from [66].*

microscopy are either too labor-intensive or insensitive, thus merging nanomaterials with biosensing technology are expected to efficiently manage TB diagnosis. Analysis of the last decade relevant literature revealed that the convergence of nanotechnology and biotechnology provides great prospects in the fabrication of new DNA nanobiosensing platforms endowed with rapidity, sensitivity, accuracy, and cost-effectiveness. Nevertheless, the existing portfolio of potential TB DNA based nanobiosensors all have their own pros and cons and they have not yet been successfully validated into marketed products that can be benchmarked. Therefore, there are still many considerable challenges and issues remained for reliable and effective use of these devices in routine clinical settings. Moreover, with the emerging lab-on-a-chip technology with biosensors as one of the component, future trends in nanodiagnostics will continue for point-of-care diagnostics with a sample-in answer-out approach that hampers user-error, thus enabling their use by nonspecialized personnel.

References

[1] WHO, World Health Organization Global Tuberculosis 2018 Report Executive Summary, WHO/CDS/TB/2018.25. (2018). Available from: who.int/tb/publications/global_report/tb18_ExecSum_web_4Oct18.pdf. Accessed 16.10.19.

[2] S. Gupta, V. Kakkar, Recent technological advancements in tuberculosis diagnostics—a review, Biosens. Bioelectron. 115 (2018) 14–29.

[3] S. Wang, F. Inci, G. De Libero, A. Singhal, U. Demirci, Point-of-care assays for tuberculosis: role of nanotechnology/microfluidics, Biotechnol. Adv. 31 (4) (2013) 438–449.
[4] B. Golichenari, K. Velonia, R. Nosrati, A. Nezami, A. Farokhi-Fard, K. Abnous, et al. Label-free nanobiosensing on the road to tuberculosis detection, Biosens. Bioelectron. 113 (2018) 124–135.
[5] L. Zhou, X. He, D. He, K. Wang, D. Qin, Biosensing technologies for *Mycobacterium tuberculosis* detection: status and new developments, Clin. Dev. Immunol. 2011 (2011) 193963.
[6] P. Martinkova, A. Kostelnik, T. Valek, M. Pohanka, Main streams in the construction of biosensors and their applications, Int. J. Electrochem. Sci. 12 (2017) 7386–7403.
[7] A. Bekmurzayeva, M. Sypabekova, D. Kanayeva, Tuberculosis diagnosis using immunodominant, secreted antigens of *Mycobacterium tuberculosis*, Tuberculosis (Edinb.) 93 (4) (2013) 381–388.
[8] O.W. Akkerman, T.S. van der Werf, M. de Boer, J.L. de Beer, Z. Rahim, J.W.A. Rossen, et al. Comparison of 14 molecular assays for detection of *Mycobacterium tuberculosis* complex in bronchoalveolar lavage fluid, J. Clin. Microbiol. 51 (11) (2013) 3505–3511.
[9] K.L. Chin, M.E. Sarmiento, M.N. Norazmi, A. Acosta, DNA markers for tuberculosis diagnosis, Tuberculosis 113 (2018) 139–152.
[10] D. Machado, I. Couto, M. Viveiros, Advances in the molecular diagnosis of tuberculosis: from probes to genomes, Infect. Genet. Evol. 72 (2019) 93–112.
[11] A. Rabti, N. Raouafi, A. Merkoçi, Bio(sensing) devices based on ferrocene-functionalized graphene and carbon nanotubes, Carbon 108 (2016) 481–514.
[12] Z. Zhu, An overview of carbon nanotubes and graphene for biosensing applications, Nano-Micro Lett. 9 (3) (2017) 25.
[13] Y. Shao, J. Wang, H. Wu, J. Liu, I.A. Aksay, Y. Lin, Graphene based electrochemical sensors and biosensors: a review, Electroanalysis 22 (2010) 1027–1036.
[14] N.F. Chiu, T.Y. Huang, C.C. Kuo, W.C. Lee, M.H. Hsieh, H.C. Lai, Single-layer graphene based SPR biochips for tuberculosis bacillus detection, Proc. SPIE 8427 (2012) 84273M–1.
[15] B.A. Prabowo, A. Alom, M.K. Secario, F.C.P. Masim, H.C. Lai, K. Hatanaka, et al. Graphene-based portable SPR sensor for the detection of *Mycobacterium tuberculosis* DNA strain, Procedia Eng. 168 (2016) 541–545.
[16] L.H. Nguyen, T.D. Nguyen, V.H. Tran, T.T.H. Dang, D.L. Tran, Functionalization of reduced graphene oxide by electroactive polymer for biosensing applications, Adv. Nat. Sci. Nanosci. Nanotechnol. 5 (2014) 035005.
[17] Y. Chen, Y. Li1, Y. Yang, F. Wu, J. Cao, L. Bai, A polyaniline-reduced graphene oxide nanocomposite as a redox nanoprobe in a voltammetric DNA biosensor for *Mycobacterium tuberculosis*, Microchim. Acta 184 (2017) 1801–1808.
[18] M.D. Mukherjee, C. Dhand, N. Dwivedi, B.P. Singh, G. Sumana, V.V. Agarwal, et al. Facile synthesis of 2-dimensional transparent graphene flakes for nucleic acid detection, Sensor Actuat. B Chem. 210 (2015) 281–289.
[19] F.S. Mohamad, M.H.M. Zaid, J. Abdullah, R.M. Zawawi, H.N. Lim, Y. Sulaiman, et al. Synthesis and characterization of polyaniline/graphene composite nanofiber and its application as an electrochemical DNA biosensor for the detection of *Mycobacterium tuberculosis*, Sensors 17 (2017) 2789.
[20] C. Liu, D. Jiang, G. Xiang, L. Liu, F. Liu, X. Pu, An electrochemical DNA biosensor for the detection of *Mycobacterium tuberculosis*, based on signal amplification of graphene and a gold nanoparticle-polyaniline nanocomposite, Analyst 139 (2014) 5460–5465.
[21] N.K. Mogha, V. Sahu, R.K. Sharma, D.T. Masram, Reduced graphene oxide nanoribbon immobilized gold nanoparticles based electrochemical DNA biosensor for detection of *Mycobacterium tuberculosis*, J. Mater. Chem. B (6) (2018) 5181–5187.
[22] V. Perumal, M. Shuaib Mohamed Saheed, N.M. Mohamed, M. Salleh Mohamed Saheed, S.S. Murthe, S.C.B. Gopinath, et al. Gold nanorod embedded novel 3D graphene nanocomposite for selective bio-capture in rapid detection of *Mycobacterium tuberculosis*, Biosens. Bioelectron. 116 (2018) 116–122.
[23] M.H.M. Zaid, J. Abdullah, N.A. Yusof, Y. Sulaiman, H. Wasoh, M.F. Md Noh, et al. PNA biosensor based on reduced graphene oxide/water soluble quantum dots for the detection of *Mycobacterium tuberculosis*, Sensor Actuat. B Chem. 241 (2017) 1024–1034.
[24] S.-H. Hwang, D.-E. Kim, H. Sung, B.-M. Park, M.-J. Cho, O.-J. Yoon, et al. Simple detection of the IS6110 sequence of *Mycobacterium tuberculosis* complex in sputum, based on PCR with graphene oxide, PLoS ONE 10 (8) (2015) e0136954.
[25] A. Oberlin, M. Endo, T. Koyama, Filamentous growth of carbon through benzene decomposition, J. Cryst. Growth 32 (1976) 335–349.
[26] S. Ijima, Helical microtubules of graphitic carbon, Nature 354 (1991) 56–58.
[27] A. Miodek, N. Mejri, M. Gomgnimbou, C. Sola, H. Korri-Youssoufi, E-DNA sensor of *Mycobacterium tuberculosis* based on electrochemical assembly of nanomaterials (MWCNTs/PPy/PAMAM), Anal. Chem. 87 (18) (2015) 9257–9264.
[28] S. Bizid, S. Blili, R. Mlika, A. Haj Said, H. Korri-Youssoufi, Direct E-DNA sensor of *Mycobacterium tuberculosis* mutant strain based on new nanocomposite transducer (Fc-ac-OMPA/MWCNTs), Talanta 184 (2018) 475–483.
[29] Y. Chen, S. Guo, M. Zhao, P. Zhang, Z. Xin, J. Tao, et al. Amperometric DNA biosensor for *Mycobacterium*

tuberculosis detection using flower-like carbon nanotubes-polyaniline nanohybrid and enzyme-assisted signal amplification strategy, Biosens. Bioelectron. 119 (2018) 215–220.
[30] B. Zribi, E. Roy, A. Pallandre, S. Chebil, M. Koubaa, N. Mejri, et al. A microfluidic electrochemical biosensor based on multiwall carbon nanotube/ferrocene for genomic DNA detection of *Mycobacterium tuberculosis* in clinical isolates, Biomicrofluidics 10 (2016) 014115.
[31] M. Das, C. Dhand, G. Sumana, A.K. Srivastava, N. Vijayan, R. Nagarajan, et al. Zirconia grafted carbon nanotubes-based biosensor for *M. tuberculosis* detection, Appl. Phys. Lett. 99 (2011) 143702.
[32] M. Holzinger, A. Le Goff, S. Cosnier, Nanomaterials for biosensing applications: a review, Front. Chem. 2 (2014) 63.
[33] G. Doria, J. Conde, B. Veigas, L. Giestas, C. Almeida, M. Assunção, et al. Noble metal nanoparticles for biosensing applications, Sensors 12 (2) (2012) 1657–1687.
[34] M.C. Daniel, D. Astruc, Gold nanoparticles: assembly, supramolecular chemistry, quantum-size-related properties, and applications toward biology, catalysis, and nanotechnology, Chem. Rev. 104 (1) (2004) 293–346.
[35] M.S. Verma, J.L. Rogowski, L. Jones, F.X. Gu, Colorimetric biosensing of pathogens using gold nanoparticles, Biotechnol. Adv. 33 (6) (2015) 666–680.
[36] P.V. Baptista, M. Koziol-Montewka, J. Paluch-Oles, G. Doria, R. Franco, Gold-nanoparticle-probe-based assay for rapid and direct detection of *Mycobacterium tuberculosis* DNA in clinical samples, Clin. Chem. 52 (7) (2006) 1433–1434.
[37] L.B. Silva, B. Veigas, G. Doria, P. Costa, J. Inácio, R. Martins, et al. Portable optoelectronic biosensing platform for identification of mycobacteria from the *Mycobacterium tuberculosis* complex, Biosens. Bioelectron. 26 (2011) 2012–2017.
[38] T. Kaewphinit, S. Santiwatanakul, K. Chansiri, Colorimetric DNA based biosensor combined with loop-mediated isothermal amplification for detection of *Mycobacterium Tuberculosis* by using gold nanoprobe aggregation, Sensors Transducers 149 (2) (2013) 123–128.
[39] I. Bernacka-Wojcik, P. Lopes, A.C. Vaz, B. Veigas, P.J. Wojcik, P. Simões, et al. Bio-microfluidic platform for gold nanoprobe based DNA detection—application to *Mycobacterium tuberculosis*, Biosens. Bioelectron. 48 (2013) 87–93.
[40] B. Veigas, P. Pedrosa, F.F. Carlos, L. Mancio-Silva, A.R. Grosso, E. Fortunato, et al. One nanoprobe, two pathogens: gold nanoprobes multiplexing for point-of-care, J. Nanobiotechnol. 13 (2015) 48.
[41] T.-T. Tsai, C.-Y. Huang, C.-A. Chen, S.-W. Shen, M.-C. Wang, C.-M. Cheng, et al. Diagnosis of tuberculosis using colorimetric gold nanoparticles on a paper-based analytical device, ACS Sens. 2 (2017) 1345–1354.
[42] H.H. Nguyen, J. Park, S. Kang, M. Kim, Surface plasmon resonance: a versatile technique for biosensor applications, Sensors 15 (5) (2015) 10481–10510.
[43] Y. Xiang, X. Zhu, Q. Huang, J. Zheng, W. Fu, Real-time monitoring of mycobacterium genomic DNA with target-primed rolling circle amplification by a Au nanoparticle-embedded SPR biosensor, Biosens. Bioelectron. 66 (2015) 512–519.
[44] M. Matsishin, A. Rachkov, A. Lopatynskyi, V. Chegel, A. Soldatkin, A. El'skaya, Selective amplification of SPR biosensor signal for recognition of rpoB gene fragments by use of gold nanoparticles modified by thiolated DNA, Nanoscale Res. Lett. 12 (2017) 252.
[45] T. Kaewphinit, S. Santiwatanakul, K. Chansiri, Gold nanoparticle amplification combined with quartz crystal microbalance DNA based biosensor for detection of *Mycobacterium Tuberculosis*, Sensors Transducers J. 146 (11) (2012) 156–163.
[46] J. Zhang, J. Huang, F. He, The construction of *Mycobacterium tuberculosis* 16S rDNA MSPQC sensor based on Exonuclease III-assisted cyclic signal amplification, Biosens. Bioelectron. 138 (2019) 111322.
[47] E. Torres-Chavolla, E.C. Alocilja, Nanoparticle based DNA biosensor for tuberculosis detection using thermophilic helicase-dependent isothermal amplification, Biosens. Bioelectron. 26 (2011) 4614–4618.
[48] C. Thiruppathiraja, S. Kamatchiammal, P. Adaikkappan, D.J. Santhosh, M. Alagar, Specific detection of *Mycobacterium* sp. genomic DNA using dual labeled gold nanoparticle based electrochemical biosensor, Anal. Biochem. 417 (2011) 73–79.
[49] X.-F. Zhang, Z.-G. Liu, W. Shen, S. Gurunathan, Silver nanoparticles: synthesis, characterization, properties, applications, and therapeutic approaches, Int. J. Mol. Sci. 17 (9) (2016) 1534.
[50] H. Wei, C. Chen, B. Han, E. Wang, Enzyme colorimetric assay using unmodified silver nanoparticles, Anal. Chem. 80 (2008) 7051–7055.
[51] R.A. Karaballi, A. Nel, S. Krishnan, J. Blackburn, C.L. Brosseau, Development of an electrochemical surface enhanced Raman spectroscopy (EC-SERS) aptasensor for direct detection of DNA hybridization, Phys. Chem. Chem. Phys. 17 (2015) 21356–21363.
[52] P. Teengam, W. Siangproh, A. Tuantranont, T. Vilaivan, O. Chailapakul, C.S. Henry, Multiplex paper-based colorimetric DNA sensor using pyrrolidinyl peptide nucleic acid-induced AgNPs aggregation for detecting MERS-CoV, MTB and HPV oligonucleotide, Anal. Chem. 89 (10) (2017) 5428–5435.
[53] H. Arami, A. Khandhar, D. Liggitt, K.M. Krishnan, In vivo delivery, pharmacokinetics, biodistribution and toxicity of iron oxide nanoparticles, Chem. Soc. Rev. 44 (2015) 8576–8607.

[54] M. Hasanzadeh, N. Shadjou, M. de la Guardia, Iron and iron-oxide magnetic nanoparticles as signal-amplification elements in electrochemical biosensing, TrAC Trends Anal. Chem. 72 (2015) 1–9.
[55] N. Prabhakar, P.R. Solanki, A. Kaushik, M.K. Pandey, B.D. Malhotra, Peptide nucleic acid immobilized biocompatible silane nanocomposite platform for *Mycobacterium tuberculosis* detection, Electroanalysis 22 (22) (2010) 2672–2682.
[56] M.P. Costa, C.A.S. Andrade, R.A. Montenegro, F.L. Melo, M.D.L. Oliveira, Self-assembled monolayers of mercaptobenzoic acid and magnetite nanoparticles as an efficient support for development of tuberculosis genosensor, J. Colloid Interf. Sci. 433 (2014) 141–148.
[57] M. Haddaoui, C. Sola, N. Raouafi, H. Korri-Youssoufi, E-DNA detection of rpoB gene resistance in *Mycobacterium tuberculosis* in real samples using Fe_3O_4/polypyrrole nanocomposite, Biosens. Bioelectron. 128 (2019) 76–82.
[58] F. Bellezza, A. Cipiciani, M.A. Quotadamo, Immobilization of myoglobin on phosphate and phosphonate grafted-zirconia nanoparticles, Langmuir 21 (24) (2005) 11099–11104.
[59] M. Das, G. Sumana, R. Nagarajan, B.D. Malhotra, Zirconia based nucleic acid sensor for *Mycobacterium tuberculosis* detection, Appl. Phys. Lett. 96 (2010) 133703.
[60] M. Das, C. Dhand, G. Sumana, A.K. Srivastava, R. Nagarajan, L. Nain, et al. Electrophoretic fabrication of chitosan-zirconium-oxide nanobiocomposite platform for nucleic acid detection, Biomacromolecules 12 (2011) 540–547.
[61] S. Barreda-García, M.J. González-Álvarez, N. de-los-Santos-Álvarez, J.J. Palacios-Gutiérrez, A.J. Miranda-Ordieres, M.J. Lobo-Castañón, Attomolar quantitation of *Mycobacterium tuberculosis* by asymmetric helicase-dependent isothermal DNA-amplification and electrochemical detection, Biosens. Bioelectron. 68 (2015) 122–128.
[62] B. Ng, E.J.H. Wee, N.P. West, M. Trau, Naked-eye colorimetric and electrochemical detection of *Mycobacterium tuberculosis*—towards rapid screening for active case finding, ACS Sensors 1 (2) (2016) 173–178.
[63] P. Fanjul-Bolado, M.B. Gonzalez-Garia, A. Costa-Garcia, Amperometric detection in TMB/HRP-based assays, Anal. Bioanal. Chem. 382 (2) (2005) 297–302.
[64] M.F. Frasco, N. Chaniotakis, Semiconductor quantum dots in chemical sensors and biosensors, Sensors 9 (9) (2009) 7266–7286.
[65] M. Gazouli, E. Liandris, M. Andreadou, L.A. Sechi, S. Masala, D. Paccagnini, et al. Specific detection of unamplified mycobacterial DNA by use of fluorescent semiconductor quantum dots and magnetic beads, J. Clin. Microbiol. (2010) 2830–2835.
[66] T.R. Shojaei, M.A.M. Salleh, M. Tabatabaei, A. Ekrami, R. Motallebi, T. Rahmani-Cherati, et al. Development of sandwich-form biosensor to detect *Mycobacterium tuberculosis* complex in clinical sputum specimens, Braz. J. Infect. Dis. 18 (6) (2014) 600–608.
[67] W. Wang, Q. Hao, W. Wang, L. Bao, J. Lei, Q. Wang, et al. Quantum dot-functionalized porous ZnO nanosheets as a visible light induced photoelectrochemical platform for DNA detection, Nanoscale 6 (2014) 2710–2717.
[68] C. Zhang, J. Lou, W. Tu, J. Bao, Z. Dai, Ultrasensitive electrochemical biosensing for DNA using quantum dots combined with restriction endonuclease, Analyst 140 (2015) 506–511.
[69] W. Kapfer, J. Walter, T.A. Trautner, Cloning, characterization and evolution of the BsuFI restriction endonuclease gene of *Bacillus subtilis* and purification of the enzyme, Nucleic Acids Res. 19 (23) (1991) 6457–6463.